

**Piezo-strain induced non-volatile resistance states in (011)-
La_{2/3}Sr_{1/3}MnO₃/0.7Pb(Mg_{2/3}Nb_{1/3})O₃-0.3PbTiO₃ epitaxial heterostructures**

Yuanjun Yang, Z. L. Luo, Meng Meng Yang, Haoliang Huang, Haibo Wang, J. Bao, Guoqiang Pan, C. Gao, Qiang Hao, Shutong Wang, Michael Jokubaitis, Wenzhe Zhang, Gang Xiao, Yiping Yao, Yukuai Liu, and X. G. Li

Citation: *Applied Physics Letters* **102**, 033501 (2013); doi: 10.1063/1.4788723

View online: <http://dx.doi.org/10.1063/1.4788723>

View Table of Contents: <http://scitation.aip.org/content/aip/journal/apl/102/3?ver=pdfcov>

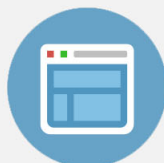
Published by the [AIP Publishing](#)

Advertisement:



Re-register for Table of Content Alerts

Create a profile.



Sign up today!



Piezo-strain induced non-volatile resistance states in (011)-La_{2/3}Sr_{1/3}MnO₃/0.7Pb(Mg_{2/3}Nb_{1/3})O₃-0.3PbTiO₃ epitaxial heterostructures

Yuanjun Yang,^{1,2,3} Z. L. Luo,¹ Meng Meng Yang,¹ Haoliang Huang,¹ Haibo Wang,¹ J. Bao,¹ Guoqiang Pan,¹ C. Gao,^{1,3,a)} Qiang Hao,² Shutong Wang,² Michael Jokubaitis,² Wenzhe Zhang,² Gang Xiao,^{2,a)} Yiping Yao,⁴ Yukuai Liu,⁴ and X. G. Li^{3,4}

¹National Synchrotron Radiation Laboratory & School of Nuclear Science and Technology, University of Science and Technology of China, Hefei, Anhui 230026, China

²Physics Department, Brown University, Providence, Rhode Island 02912, USA

³CAS Key Laboratory of Materials for Energy Conversion, Department of Materials Science and Engineering, University of Science and Technology of China, Hefei, Anhui 230026, China

⁴Hefei National Laboratory for Physical Sciences at Microscale & Department of Physics, University of Science and Technology of China, Hefei, Anhui 230026, China

(Received 12 October 2012; accepted 3 January 2013; published online 22 January 2013)

The non-volatile resistance states induced by converse piezoelectric effect are observed in ferromagnetic/ferroelectric epitaxial heterostructures of (011)-La_{2/3}Sr_{1/3}MnO₃/0.7Pb(Mg_{2/3}Nb_{1/3})O₃-0.3PbTiO₃ (LSMO/PMN_{0.7}PT_{0.3}). Three stable remnant strain states and the corresponding resistance states are achieved by properly reversing the electric field from the depolarized direction in ferroelectric PMN_{0.7}PT_{0.3} substrate. The non-volatile resistance states of the LSMO film can be manipulated by applied electric-field pulse sequence as a result of the large coupling between the electronic states of LSMO film and the strain transferred from the ferroelectric substrate. The electrically tunable, non-volatile resistance states observed exhibit potential for applications in low-power-consumption electronic devices. © 2013 American Institute of Physics.

[<http://dx.doi.org/10.1063/1.4788723>]

Perovskite manganites that are rich in exotic electronic states due to the strong coupling between electron spin, charge, and orbital degrees of freedom have stimulated intensive research activity in recent years, both as a platform for basic physics and for potential applications in spintronic devices.¹⁻⁴ In particular, La_{2/3}Sr_{1/3}MnO₃ (LSMO) is an attractive material as it displays colossal magnetoresistance,⁵ half-metallicity,⁵ and room temperature ferromagnetism.⁶ The transport and magnetic properties of LSMO epitaxial films can be modulated by externally applied fields, such as electric fields^{1,3} and magnetic fields.⁵ Moreover, recent research has shown that inherent epitaxial strain inside LSMO films can effectively control its electronic properties.⁷ It has been reported that Curie temperature (T_c) can be controlled via biaxial strain through the influence of the Jahn-Teller (JT) effect in (001)-La_{0.7}Sr_{0.3}MnO₃ epitaxial films deposited on various substrates.⁸ The temperature dependence of the resistivity and magnetoresistance are also strongly affected by the tensile tetragonal distortion in LSMO thin films.⁹ So far, static strain in LSMO films has been generated through the use of different substrates. However, there is increasing interest in dynamic strain control in LSMO films by using external electric field, as was first proposed by Schultz¹⁰ and Zheng¹¹ *et al.*, and experimentally demonstrated in (001)-La_{0.7}Sr_{0.3}MnO₃ film grown on 0.7Pb(Mg_{2/3}Nb_{1/3})O₃-0.3PbTiO₃ (PMN-PT) ferroelectric substrates.¹⁰⁻¹³

However, the magnetization and resistance states of the LSMO films developed to date return to their original state

once the external electric field is removed. Thus, producing multiple persistent and reversible strain states in LSMO/PMN_{0.7}PT_{0.3} structure could be beneficial to non-volatile memory applications;¹⁴⁻²⁰ using an electric field to induce remnant strain states would consume less power than comparable electrical-current-driven magnetic random access memories (MRAM).^{15,20} With this motivation, we have developed a heterostructure of LSMO/PMN_{0.7}PT_{0.3} that exhibits multiple remnant strain and resistance states, which may be switched by an electric field pulse. The coupling between the strain and resistance states is mediated by the double exchange interaction between Mn³⁺ and Mn⁴⁺ sites, which is controllable by an electric field applied to the LSMO/PMN_{0.7}PT_{0.3} structure.

Using RF sputtering, we deposited 80 nm-thick LSMO epitaxial films¹³ on a (011) PMN_{0.7}PT_{0.3} single crystal substrate²¹ with a dimension of 5 mm $\langle 0\bar{1}1 \rangle \times 5.5$ mm $\langle 100 \rangle \times 0.55$ mm $\langle 011 \rangle$. The films were annealed in an O₂ atmosphere at 850 °C to release the initial strain¹³ and to improve crystallinity.¹³ A 300 nm-thick Au film was sputtered on the backside of the substrate as the bottom electrode. The front-side of the LSMO film served as the top electrode. The in-plane strain of the sample was measured using a strain gauge bonded on a separate PMN_{0.7}PT_{0.3} substrate (5 mm $\langle 0\bar{1}1 \rangle \times 5.5$ mm $\langle 100 \rangle \times 0.7$ mm $\langle 011 \rangle$). The epitaxial nature of the LSMO film was confirmed using the high resolution synchrotron radiation X-ray diffraction (XRD) device on Hefei Light Source and Shanghai Synchrotron Radiation Facility.¹³ To check the initial strain in the LSMO film, we performed reciprocal space mapping around the (103) peaks. Fig. 1(a) shows the (103) diffraction peak of the LSMO/PMN_{0.7}PT_{0.3}

^{a)} Authors to whom correspondence should be addressed. Electronic addresses: cgao@ustc.edu.cn and gang_xiao@brown.edu.

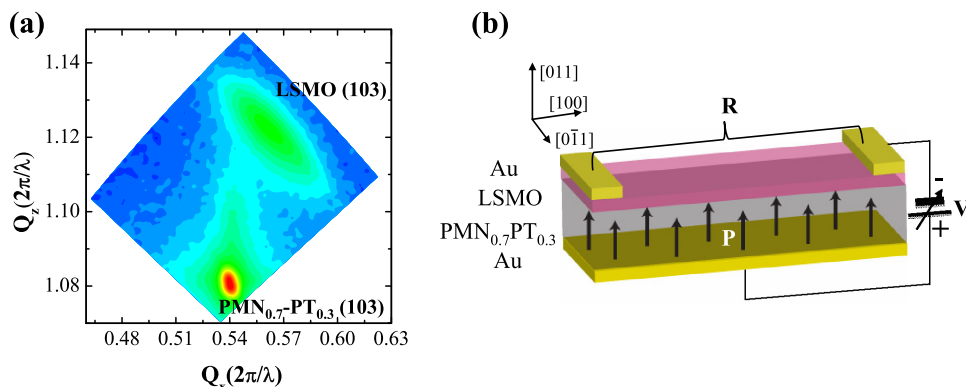


FIG. 1. (a) Reciprocal space mapping (103) diffraction peaks of (011)-LSMO/PMN_{0.7}PT_{0.3} epitaxial heterostructures. (b) The schematic of the resistance measurement with the field-effect configuration.

epitaxial film used for our study. From Fig. 1(a), the in-plane (Q_x) and out-of-plane (Q_z) lattice constants (a and c) of the LSMO film were calculated to be 0.388 nm, which is close to the bulk pseudocubic lattice constant (0.387 nm) of LSMO (at a Sr-doping of 0.33).⁹ Therefore, the initial strain due to lattice mismatch and thermal treatment could be neglected reasonably in this paper.

We measured the resistance of the LSMO film along the in-plane [100] direction as we subjected the substrate to a biasing electrical field (voltage), using a field-effect transport

device^{10,22} as shown in Fig. 1(b). The positive polarized state is defined to lie along the direction from the bottom to the top electrode. Fig. 2 shows the relative resistance change $\Delta R/R$ along the [100] direction of the LSMO film and the in-plane strains ($[0\bar{1}1]$ and $[100]$) in the substrate as functions of the applied, cycling bipolar electric field. It can be seen that the resistance change is intimately related to the induced strains in the film. The magnitude of the resistance change ($\Delta R/R \sim 1\%$) in the top of Fig. 2 is comparable to what has been observed by others in similar structures.^{10,11} We observed giant tensile strain values along the $[0\bar{1}1]$ direction (on the order of 1500 ppm) at the coercive fields, $E_{c1} \sim +1.3$ kV/cm and $E_{c2} \sim -1.7$ kV/cm, as shown in the middle of Fig. 2, indicating the high quality of the ferroelectric substrate. The compressive strain values along the [100] direction are smaller at about -600 ppm as shown in the bottom of Fig. 2. Here, the observed double strain peaks around E_{c1} and E_{c2} were caused by rotation of the polarization vector.^{15,23} In both cases, when the external electric field is reduced to zero, there are no remnant strain states. Consequently, there are no remnant resistance states either.

Next, we cycled the electric field between the maximums of -3 kV/cm and $+1.3$ kV/cm, which are just below the coercive field E_{c1} . As shown in Fig. 3, hysteresis loops with a remnant strain state at zero field were created, with the $[0\bar{1}1]$ strain at $+1200$ ppm and the [100] strain at -380 ppm. We will refer to this field cycling as negative cycling below.

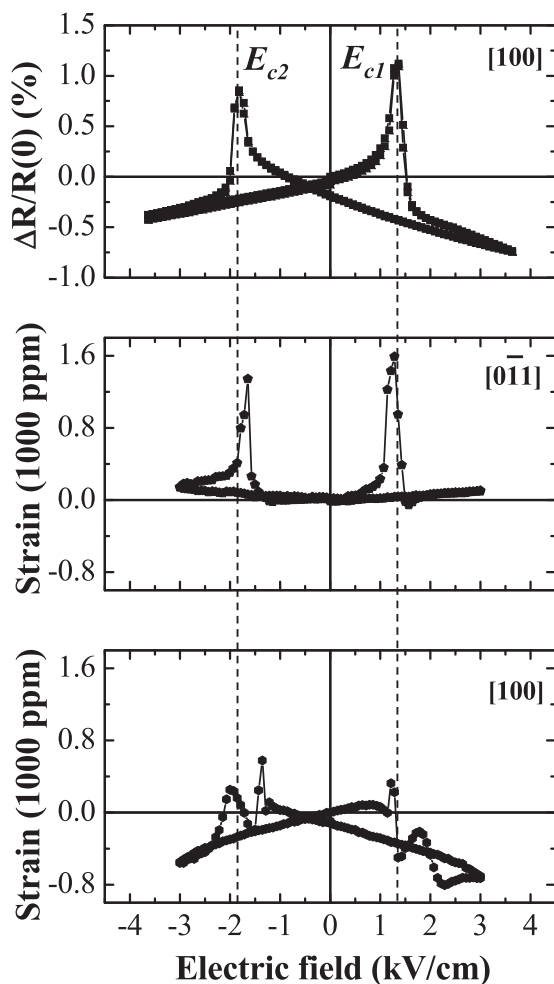


FIG. 2. The resistance change (up) is a function of electric field. The strains along the $[0\bar{1}1]$ (middle) and [100] (bottom) directions vs electric field with saturated poling of the PMN_{0.7}PT_{0.3} substrate. $\Delta R/R = ((R(E) - R(0))/R(0))$, where $R(E)$ and $R(0)$ are the resistance of the LSMO film under an electric field E and zero, respectively.

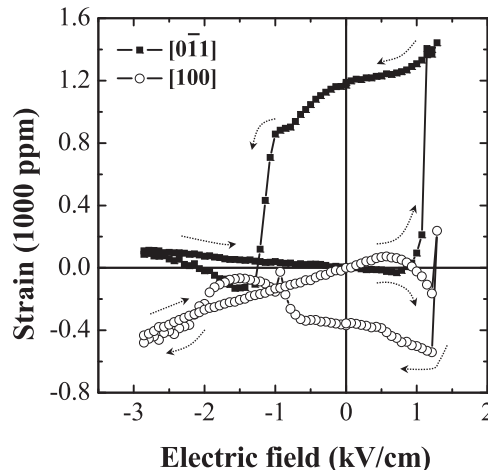


FIG. 3. The strains states along the [100] and $[0\bar{1}1]$ direction with partially positive poling from negatively poled state of the PMN_{0.7}PT_{0.3} substrate. The arrows show the cycling direction of the electric field.

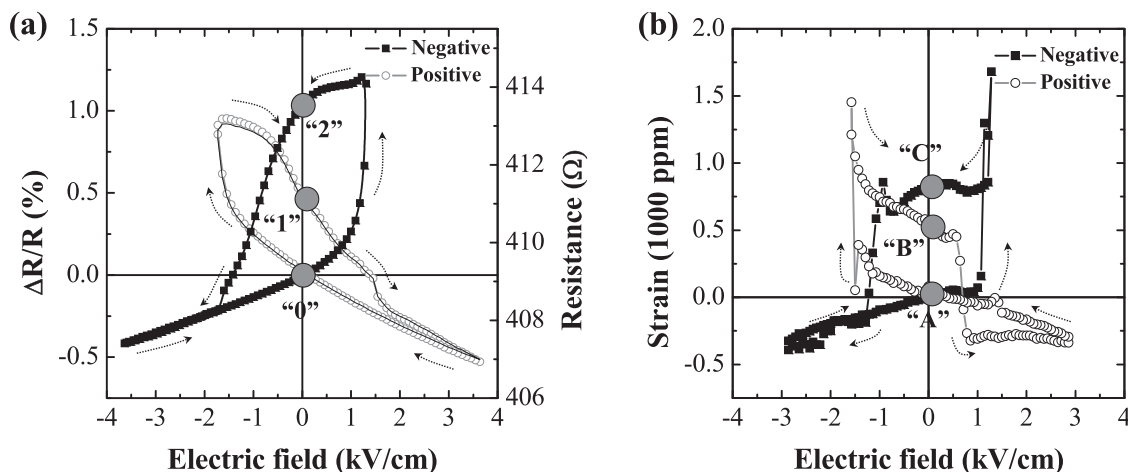


FIG. 4. (a) The resistance change hysteresis under the negatively and positively partially poled states. The right axis shows the corresponding resistance. The gray solid circles mark the remnant resistance states “0,” “1,” and “2.” (b) The corresponding total in-plane strain hysteresis by cycling negative and positive electric field. The remnant strain states “A,” “B,” and “C” are also marked.

Similarly, we cycled between the maximum positive field and a negative field close to E_{c2} (to be referred to as positive cycling). We obtained similar hysteresis loops (not shown). Taken together, this technique is called ferroelectric domain engineering for creating the non-volatile remnant strain states in ferroelectric materials.^{15,18,23} This unique and giant remnant strain mainly originates from the non 180° ferroelectric polarization reorientation in [011]-poled relaxor ferroelectrics $\text{PMN}_{1-x}\text{PT}_x$ ($x \sim 0.28-0.33$, around the morphotropic phase boundary (MPB)).^{18,23}

Correspondingly, we show the resistance hysteresis loops for both negative and positive field cycling are shown in Fig. 4(a). These results exhibit several key features. First, the initial resistance state, denoted as “0” in Fig. 4(a), remains the same regardless of positive or negative field saturation. Second, there exist two remnant resistance states (see states “1” and “2” in Fig. 4(a)) that have resistances different from that of the “0” state. Interestingly, the resistance memory effect shown in Fig. 4(a), although qualitatively similar, depends on the type of cycling (negative or positive). All three fixed resistance states, “0,” “1,” and “2,” can be accessed by manipulating the field cycling.

The hysteretic resistance behavior in Fig. 4(a) is a result of the total in-plane strain of the $\text{PMN}_{0.7}\text{PT}_{0.3}$ substrate. Here, the total in-plane strain is defined as the sum of strains along

the two perpendicular directions [100] and $[0\bar{1}1]$ as shown in Fig. 3. Under the volume conservation assumption of unit cell, total in-plane strain is a measure of the out-of-plane strain. Fig. 4(b) shows the total in-plane strain for both the negative and positive field cycling. Qualitatively, the relative resistance change depends on the total in-plane strain. A positive total strain leads a positive relative resistance change, and vice versa. Also, the three remnant strain states (“A,” “B,” and “C”) yield three remnant resistance states (“0,” “1,” and “2”).

The strain-induced resistance modulation shown in Fig. 4(a) can be understood in terms of the intrinsic double-exchange interaction, which is strongly influenced by the in-plane strain. A positive strain increases the Mn-O bond length and decreases the itinerant electron hopping strength between the Mn^{3+} and Mn^{4+} sites,^{22,24-26} thereby enhancing the resistivity of the LSMO film.^{25,26}

The remnant strain and resistance states observed in our composite structures have important implications for non-volatile memory applications.²⁷ Based on Figs. 4(a) and 4(b), we can change the remnant resistance state of the LSMO film by applying an electric field pulse to the structure. For example, as shown in Fig. 5(a), by applying a sequence of (larger) positive electric field pulses and (smaller) negative pulses, corresponding binary “0,” “1” resistance states can be generated or stored. Similarly, in Fig. 5(b), a sequence of (larger)

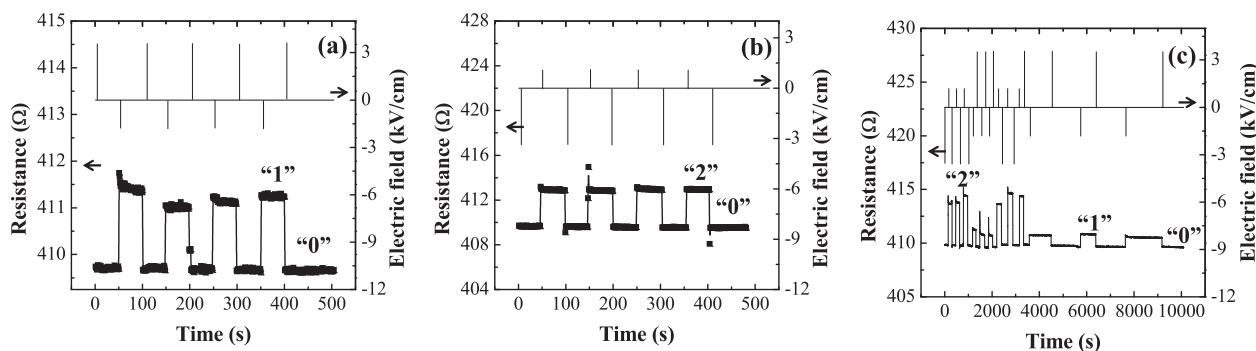


FIG. 5. (a) The non-volatile resistance states “0” and “1” are switched by a sequence of larger positive pulses (up) field $+3.27$ kV/cm and -1.72 kV/cm. (b) The non-volatile resistance states “0” and “2” are switched by a sequence of stronger negative pulses -3.27 kV/cm and $+1.31$ kV/cm. (c) The ternary non-volatile resistance states “0,” “1,” and “2” are switched among each other under the designed pulsing sequence (up) combined by $+3.27$ kV/cm, -1.72 kV/cm, -3.27 kV/cm, and $+1.31$ kV/cm.

negative pulses and (smaller) positive pulses generates binary “0,” “2” resistance states. Finally, as shown in Fig. 5(c), a tailored pulse sequence allows us to encode ternary resistance states of “0,” “1,” and “2”. Therefore, our composite structure can store non-volatile information in the form of electric field-induced remnant strain, and read the same information from the remnant resistances. Crucially, the information extraction process is not destructive to the existing remnant state, unlike non-volatile ferroelectric random access memory (FeRAM).²⁸

In summary, the remnant strain states of the LSMO/PMN_{0.7}PT_{0.3} epitaxial heterostructure are obtained by ferroelectric domain engineering. The corresponding remnant resistance states are found to be reversible and non-volatile, and can be switched among the ternary states “0,” “1,” and “2” with the application of a pulsed electric field sequence. The modulation of the resistance of an LSMO film by an electric field is attributed to the varying hopping strength of itinerant electrons between the Mn³⁺ and the Mn⁴⁺ sites as influenced by the induced strain. Our results provide the basis for one form of nonvolatile solid-state memory, in which information is stored in an electric field-induced remnant strain and read by inferring the remnant electrical resistance state.

This work was supported in part by the National Basic Research Program of China (973 Program) (2012CB922004/3, 2010CB934501, and 2009CB929502), the Natural Science Foundation of China (11179008, 50832005, and 51021091) and the Chinese Universities Scientific Fund, and in part by the US National Science Foundation (NSF) under Grant No. DMR-0907353. Beamtimes from NSRL and SSRF are highly appreciated.

¹S. M. Wu, S. A. Cybart, P. Yu, M. D. Rossell, J. X. Zhang, R. Ramesh, and R. C. Dynes, *Nature Mater.* **9**, 756 (2010).

²T. Yajima, Y. Hikita, and H. Y. Hwang, *Nature Mater.* **10**, 198 (2011).

³A. Chanthbouala, A. Crassous, V. Garcia, K. Bouzehouane, S. Fusil, X. Moya, J. Allibe, B. Dlubak, J. Grollier, S. Xavier, C. Deranlot, A. Moshar, R. Proksch, N. D. Mathur, M. Bibes, and A. Barthelémy, *Nat. Nanotechnol.* **7**, 101 (2012).

⁴Q. P. Chen, J. J. Yang, Y. G. Zhao, S. Zhang, J. W. Wang, M. H. Zhu, Y. Yu, X. Z. Zhang, Z. Wang, B. Yang, D. Xie, and T. L. Ren, *Appl. Phys. Lett.* **98**, 172507 (2011).

⁵J.-H. Park, E. Vescovo, H.-J. Kim, C. Kwon, R. Ramesh, and T. Venkatesan, *Nature* **392**, 794 (1998).

⁶G. H. Jonker and J. H. van Santen, *Physica* **16**, 337 (1950).

⁷A. Vailionis, H. Boschker, W. Siemons, E. P. Houwman, D. H. A. Blank, G. Rijnders, and G. Koster, *Phys. Rev. B* **83**, 064101 (2011).

⁸C. Adamo, X. Ke, H. Q. Wang, H. L. Xin, T. Heeg, M. E. Hawley, W. Zander, J. Schubert, P. Schiffer, D. A. Muller, L. Maritato, and D. G. Schlom, *Appl. Phys. Lett.* **95**, 112504 (2009).

⁹F. Yang, N. Kemik, M. D. Biegalski, H. M. Christen, E. Arenholz, and Y. Takamura, *Appl. Phys. Lett.* **97**, 092503 (2010).

¹⁰C. Thiele, K. Dörr, S. Fähler, L. Schultz, D. C. Meyer, A. A. Levin, and P. Paufler, *Appl. Phys. Lett.* **87**, 262502 (2005).

¹¹R. K. Zheng, Y. Wang, H. L. W. Chan, C. L. Choy, and H. S. Luo, *Phys. Rev. B* **75**, 212102 (2007).

¹²C. Thiele, K. Dörr, O. Bilani, J. Rödel, and L. Schultz, *Phys. Rev. B* **75**, 054408 (2007).

¹³Y. Yang, M. M. Yang, Z. L. Luo, H. Huang, H. Wang, J. Bao, C. Hu, G. Pan, Y. Yao, Y. Liu, X. G. Li, S. Zhang, Y. G. Zhao, and C. Gao, *Appl. Phys. Lett.* **100**, 043506 (2012).

¹⁴A. Brandlmaier, S. Geprags, G. Woltersdorf, R. Gross, and S. T. B. Goennenwein, *J. Appl. Phys.* **110**, 043913 (2011).

¹⁵T. X. Nan, Z. Y. Zhou, J. Lou, M. Liu, X. Yang, Y. Gao, S. Rand, and N. X. Sun, *Appl. Phys. Lett.* **100**, 132409 (2012).

¹⁶C.-Jui Hsu, J. L. Hockel, and G. P. Carman, *Appl. Phys. Lett.* **100**, 092902 (2012).

¹⁷S. Zhang, Y. G. Zhao, P. S. Li, J. J. Yang, S. Rizwan, J. X. Zhang, J. Seidel, T. L. Qu, Y. J. Yang, Z. L. Luo, Q. He, T. Zou, Q. P. Chen, J. W. Wang, L. F. Yang, Y. Sun, Y. Z. Wu, X. Xiao, X. F. Jin, J. Huang, C. Gao, X. F. Han, and R. Ramesh, *Phys. Rev. Lett.* **108**, 137203 (2012).

¹⁸T. Wu, A. Bur, P. Zhao, K. P. Mohanchandra, K. Wong, K. L. Wang, C. S. Lynch, and G. P. Carman, *Appl. Phys. Lett.* **98**, 012504 (2011).

¹⁹M. Liu, S. Li, O. Obi, J. Lou, S. Rand, and N. X. Sun, *Appl. Phys. Lett.* **98**, 222509 (2011).

²⁰J.-Mian Hu, Z. Li, L.-Qing Chen, and C.-Wen Nan, *Adv. Mater.* **24**, 2869 (2012).

²¹H. S. Luo, G. S. Xu, H. Q. Xu, P. C. Wang, and Z. W. Yin, *Jpn. J. Appl. Phys., Part 1* **39**, 5581 (2000).

²²R. K. Zheng, Y. Jiang, Y. Wang, H. L. W. Chan, C. L. Choy, and H. S. Luo, *Phys. Rev. B* **79**, 174420 (2009).

²³T. Wu, P. Zhao, M. Bao, A. Bur, J. L. Hockel, K. Wong, K. P. Mohanchandra, C. S. Lynch, and G. P. Carman, *J. Appl. Phys.* **109**, 124101 (2011).

²⁴J.-Mian Hu, Z. Li, L.-Qing Chen, and C.-Wen Nan, *Nat. Commun.* **2**, 553 (2011).

²⁵R. K. Zheng, H.-U. Habermeier, H. L. W. Chan, C. L. Choy, and H. S. Luo, *Phys. Rev. B* **80**, 104433 (2009).

²⁶J. Wang, F. X. Hu, L. Chen, J. R. Sun, and B. G. Shen, *J. Appl. Phys.* **109**, 07D715 (2011).

²⁷Y. Yang, Z. L. Luo, H. Huang, Y. Gao, J. Bao, X. G. Li, S. Zhang, Y. G. Zhao, X. Chen, G. Pan, and C. Gao, *Appl. Phys. Lett.* **98**, 153509 (2011).

²⁸M. Dawber, K. M. Rabe, and J. F. Scott, *Rev. Mod. Phys.* **77**, 1083 (2005).